CERES TRMM-PFM-VIRS Edition1 SSF Cloud Properties - Accuracy and Validation

This section discusses the spectral radiances and cloud parameters associated with the SSF data set version Edition1. The cloud parameters in the SSF are the result of convolving the values for the clear-sky and cloudy data derived for each 2-km VIRS pixel within a CERES footprint. (See Spatial matching of imager properties and broadband radiation.) Consult the SSF Collection Guide for information on how clear sky and cloud data are stored on the SSF product.

Five radiances taken at 0.67, 1.6, 3.7, 10.8, and 12.0 µm, channels 1 through 5, respectively, are measured for each VIRS pixel. Based on the values of these radiances, each VIRS pixel is classified as clear, cloudy, bad data, or no retrieval. Each clear or cloudy pixel is categorized as weak or strong to indicate the degree of confidence in the selection. Clear pixels can also have an additional classifier, either snow, aerosol, smoke, fire, sunglint, or shadow. The cloudy pixels can also have a sunglint sub-classification meaning that they were detected at angles favorable for the viewing of specular reflection from the surface. Atmospheric profiles of temperature, ozone, and humidity, model estimates of surface skin temperature (see MOA description), elevation, and one of the twenty surface types (CERES Surface Properties Home Page) are also associated with each VIRS pixel.

The 10.8 µm surface skin temperature is computed for each clear pixel while the following values are computed for each cloudy pixel: phase (ice or water); visible (0.67 µm) optical depth (τ); infrared (10.8 µm) emissivity; liquid or ice water path WP; effective droplet radius r_e or effective ice crystal diameter D_e; cloud-top pressure; effective cloud height, pressure, and temperature; and cloud-base pressure. Nominally, cloud phase and effective particle sizes are computed separately using the 1.6 and 3.7 µm channels. However, only the 3.7 µm results are included in Edition 1.

The bad-data pixels are those having at least one radiance that was set to a default value or out of the allowed range. The greatest problem causing bad data was the saturation of the thermal channels over land. The saturation temperatures for the VIRS Version 5 are 321.4, 324.9, and 319.4 K for channels 3, 4, and 5, respectively. Because of its relatively low maximum temperature and its reflected solar component, the 3.7 µm channel was often saturated during midday over deserts and scrubland. To acquire as many clear pixels as possible, it was assumed that saturated 3.7 µm pixels over land or desert were actually clear if there was no saturation in the other channels and the 10.8 µm temperature was greater than 300 K. The 3.7 µm temperature was set to the maximum temperature. If these conditions were not met, then a bad data classification was assigned to the pixel. No-retrieval pixels are those that are initially identified as cloudy, but their radiances cannot be interpreted with the theoretical models used to derive cloud particle size and optical depth.

VIRS Data

The cloud parameters rely on accurately calibrated imager radiances. VIRS Version 5 radiance data are used for Edition1. The VIRS thermal infrared channels are calibrated with onboard blackbodies and the solar channels are calibrated approximately once per month using a solar-viewing diffuser. Space looks provide zero radiance levels for the calibrations. Barnes et al. (2000) and Lyu et al. (2000) summarize the operational VIRS calibrations. The nominal VIRS calibrations were compared to other calibrated satellite data to determine stability and relative gains to determine any inconsistencies with other commonly used imagers. During the first 8 months, corresponding to the longest period of continuous CERES-PFM data, the VIRS solar and infrared channels were linearly correlated with the CERES SW and LW radiances, respectively, taken each day over ocean, land, and desert areas separately using three solar zenith angle (SZA) ranges to produce a slope for each data category. A time series of these slopes was used to monitor any trends in the imager calibrations assuming stability in the CERES reference dataset. It is assumed that the data taken over ocean are the most reliable because of the spectral homogeneity of the surface reflectance and temperature. The imagers were also compared to collocated and co-angled radiances (Nguyen et al. 1999) from the NOAA-14 Advanced Very High Resolution Radiometer (AVHRR; occasional during 1998), the eastern Geostationary Operational Environmental Satellite (GOES-8; continuous from Jan. 1998 - July 2000), the ERS-2 Along Track Scanning Radiometer (ATSR-2; two periods: Jan - Aug 1998 and Feb. - July 2000), and the MODIS Airborne Simulator (MAS; Jan. 25, 1999 over Amazon Basin) on the ER-2 aircraft. The GEOS-8 was calibrated against the NOAA-14 AVHRR on a monthly basis since 1995 to establish a trend line in the GOES gain. Thus, comparison of GOES and VIRS is equivalent to comparing AVHRR and VIRS over ocean. Spectral differences were normalized for all of the imager comparisons. The calibration studies for each channel are summarized below.

Ch. 1, VIS (0.64 µm): Reflectance R is the quantity used in the analyses. It is the ratio of the measured radiance L to the solar constant S adjusted for the normalized Earth-Sun distance d and the cos(SZA). The solar constant used here is S1 = 531.7 W $m^{-2}µm^{-1}$ sr^{-1} and the channel 1 radiance is L1.

```
CERES SW:     LSW = G * L1 + I;
```

No statistically significant trend in G found for any SZA range. Only values for ocean at SZA > 45° given, G = 0.646 µm, I = 0.

```
GOES-8 VIS:     LG = G * L1 + I;

1998 - 2000:     G = 0.004184 * M + 0.818;     I = 0,
```

where M is the number of months past January 1, 2000. This result can be compared to the trend line based on the AVHRR radiance:

```
G = 0.005553 * M + 0.797.

AVHRR VIS:  G = 0.971;      I = -2.012       (April 1998)

ATSR2 VIS:              LA = G* L1 + I

1998:  G = 0.977;        I = 0.00;          N = 392.

2000:  G = 0.970;        I = 0.00;          N = 130.

MAS VIS:                LM = G * L1 + I

1999:  G = 1.189;        I = 0.0027;        N = 114.
```

The CERES and ATSR2 results indicate that the VIRS VIS gain is not drifting with time. This result is consistent with Lyu et al. (2000), however, the MAS VIS comparison suggests that the VIRS gain is too low by roughly 18%. Initial comparisons of the comparable MODIS channel with the collocated VIRS VIS data indicate that the MAS channel is incorrect in this instance. Therefore, it is concluded that the VIRS VIS gain has not changed significantly during its first 3 years of operation. However, using the GOES-8 as a surrogate for the NOAA-14 AVHRR, it clear that the VIRS and AVHRR calibrations differ by a steadily changing amount. At launch, the VIRS radiances were 2.3% greater than their AVHRR counterparts (consistent with the direct comparison between AVHRR and VIRS). By May 1999, the two channels agreed, and by December 2000, the AVHRR radiances are 2.3% greater than the AVHRR radiances. Without an adjustment, the VIS radiances from the two instruments will continue to diverge. Although the accuracy relative to other imagers is relatively straightforward, the absolute accuracy of the VIRS VIS calibration is difficult to determine. The ATSR-2 radiances average 2.7% less than VIRS, while the MODIS reflectances average only 0.6% less than VIRS. Thus, only one or none of the diffuser-calibrated imagers can be absolutely accurate although all appear to be reasonable.

Ch. 2, NIR (1.62 µm): The NIR channel was corrected for contamination by thermal radiation at 5.2 µm because of imperfections in the instrument filter. The corrected radiance is

```
L2 = L2 - DL2,

where

DL2 = S2 * [-226.3 + 157.1*L4 - 304.9*(L4-L5) + 0.453*VZA - 0.0240*VZA^2] / 100,
```

L2, L4, and L5 are the measured radiances for channels 2, 4, and 5, respectively, and S2 is the solar constant for channel 2 (78.30 W $m^{-2} \mu m^{-1} sr^{-1}$). The formula for DL2 was developed empirically by Alexander Ignatov (Ignatov and Stowe, 2000) and is in good agreement with theoretical estimates. This correction does not account for variations in the surface emissivity so that it may be in error by 10-15% over some surfaces resulting in an overall NIR radiance error of ~0.2%. This error is generally not significant except for possibly some low-reflectance scenes such as clear ocean.

```
CERES SW:         LSW = G * L2 + I;
```

No statistically significant trend in G was found during first 8 months for SZA < 45° and for SZA > 60°. A significant degradation in the gain of 1%/month was found for 45° < SZA < 60°. However, the length of record does not eliminate the potential for a seasonal cycle. For ocean, SZA > 45°, G = 6.82 µm, I = 0.

```
ATSR-2 NIR:            LA = G * L2 + I

1998:  G = 1.171;        I = 0.000;        N = 392.

2000:  G = 1.168;        I = 0.000;        N = 130.

MAS NIR:               LM = G * L2 + I
```

```
1999:  G = 1.215         I = 0;            N = 114.
```

In this instance, the VIRS reflectances are consistently 17% lower than the ATSR-2. This result is supported by the MAS comparison. Additionally, the evidence for a trend is only found in one of the SZA ranges. Given these results and those of Lyu et al. (2000), it is concluded that there is no significant trend in the VIRS NIR gain. The large gain differences between VIRS and the ATSR-2 and MAS results are supported by a comparison of cloud droplet sizes retrieved using channels 2 and 3. The NIR-derived particle sizes were much larger than their 3.8 µm counterparts using the nominal calibration but were in excellent agreement using the ATSR-2 gains. Thus, it was concluded that additional correction must be applied to the NIR radiance. The values used here are

```
L2 = 1.17 L2.
```

Ch. 3, SIR (3.78 µm): The SIR channel measures both thermal emitted and solar reflected radiation. The radiance can be converted to an equivalent blackbody temperature T using the Planck function evaluated at the nominal channel wavelength. All solar radiation components of the measured radiance are taken into account using the channel 3 solar constant S3 = 3.428 W m^{-2} μm^{-1} sr^{-1}, a value equivalent to a blackbody temperature of 355.4 K at 3.78 µm.

```
CERES LW:              LW = G * L2 + I;
```

The LW-SIR regressions used nighttime data only. A statistically significant trend in G of 0.8%/mo was found during first 8 months. The mean value of G is 117.0 µm. However, the length of record does not eliminate the potential for a seasonal cycle.

```
ATSR-2 SIR:            TA = G * T3+ I

1998:  G = 0.9986;      I = 0.0000;                N = 392.

2000:  G = 1.0002;      I = 0.0000                 N = 130.
```

The ATSR-2 results show no trend over a 2-year period. Given these results and those of Lyu et al. (2000), it is assumed here that channel 3 has no significant variation of G with time.

```
Ch. 4, IR (10.75 µm):

CERES LW:             LLW = G * L4 + I;
```

No statistically significant trend in G was found during the first 8 months for either daytime or nighttime. The mean daytime and nighttime values of G are 7.53 µm and 7.60 µm, respectively.

```
ATSR-2 IR:             TA = G * T4 + I

1998:  G = 0.9997;      I = 0.0000;      N = 392.

2000:  G = 0.9981;      I = 0.0000;      N = 130.
```

Given these results and those of Lyu et al. (2000), it is assumed here that channel 4 has no significant variation of G with time.

```
Ch. 5, WS (11.95 µm):

CERES LW:             LLW = G * L5 + I;
```

No statistically significant trend in G was found during the first 8 months for either daytime or nighttime. The mean daytime and nighttime values of G are 8.65 µm and 8.85 µm, respectively.

```
ATSR-2 WS:              TA = G * T5 + I

1998:  G = 1.0013;       I = 0.0000;      N = 392.

2000:  G = 1.0010;       I = 0.0003;      N = 130.
```

Given these results and those of Lyu et al. (2000), it is assumed here that channel 5 has no significant variation of G with time.

Cloud Parameters

Preliminary assessment of the uncertainties in some of the cloud parameters has been completed. Many other datasets must be compared with the CERES VIRS cloud analyses before final error numbers are assigned. The cloud parameters have been evaluated visually by comparing a large number of high-resolution images with pictures of derived cloud parameters over a selected number of regions to ensure that the results appear to be qualitatively consistent with the imagery. Some of the parameters have been compared with climatological values to obtain a rough quantitative evaluation. The results have also been averaged for various surface types and angular ranges to determine any systematic variability. Many of these studies were performed prior to the finalization of the Edition1 algorithm. Thus, some of the results may no longer be completely valid. Much additional work needs to be performed and the original studies need to be repeated using the Edition1 results. The most quantitative evaluations use estimates of similar quantities derived from passive and active radiometric measurements at surface sites, in particular, the ARM Southern Great Plains (SGP) facility in central Oklahoma. The available results have been compared with the Edition1 quantities. For comparisons to ARM data, VIRS cloud properties were averaged over a 30 km square box centered on the ARM site. ARM cloud properties were averaged for 30 minutes centered on the TRMM overpass time.

Cloud amount - Figure 1 shows the comparison of mean zonal cloud amounts from VIRS for July 1998 and from surface observations for the period from 1971 - 1996. The VIRS zonal means are within + 5.3% of the climatological values from the surface. The VIRS cloud amounts are based on an earlier version of the CERES cloud mask. It is expected that cloud amounts will increase slightly in the Edition1 results because of recent improvements in low cloud detection. The results in Figure 1 demonstrate that the retrievals from CERES are reasonable as do the image evaluations. More quantitative direct comparisons with coincident surface observations, both subjective and objective will be used to provide a more quantitative assessment of the cloud amount uncertainties.

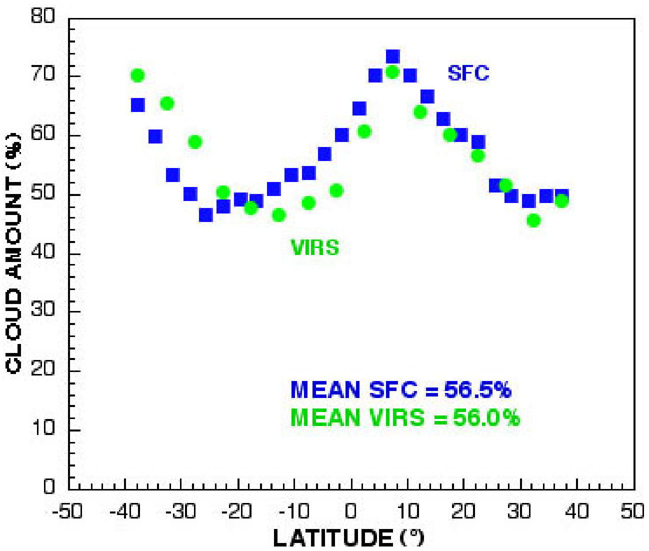

Figure 1. Comparison of mean cloud fraction from surface observations for July 1971-1992 to VIRS-retrievals for July 1998.

Cloud phase - This parameter is more difficult to evaluate because it requires either in situ or combinations of passive and active remote sensing data. Inspection of the results with coincident imagery indicates that, during the daytime, the cirrus clouds, even very thin ones, are generally identified as ice clouds. The edges of these clouds are occasionally classified as water clouds and the very thin cirrus over low clouds are sometimes classified as water clouds. At night, the phase classification is less reliable except when the cloud temperature is < 233K (ice) or > 273K (liquid). The fraction of ice clouds from VIRS relative to the total for July 1998 is 33.0% over ocean. This value is extremely close to the mean value of 33.4% derived long-term (1952-1981) surface observations (Warren et al. 1988) where cirrus and cumulonimbus are assumed to be ice clouds. Future assessments of cloud phase will use direct comparisons with remotely sensed data from the surface.

Cloud height, pressure, temperature - These parameters are all related because the cloud temperature is used to ascertain cloud height and the height is used to select the pressure. Effective cloud height derived from VIRS should be an altitude somewhere between the top and base of the cloud. It corresponds to the mean radiating temperature of the cloud. For water clouds, it is usually within a few 100 m of the top. For cirrus clouds, it can be close to the cloud base or near cloud top depending on the density of the cloud. Initial comparisons with the radar observations over the ARM site are summarized in Table 1 for cloud height and temperature. During both daytime and nighttime, the mean cloud height is always between the mean and the top altitudes derived from the surface data where the mean is average of the top and base from the radar data. The CERES algorithm was also used to estimate cloud height from Geostationary Operational Environmental Satellite (GOES) data over the southeastern Pacific where strong temperature inversions occur and the numerical weather analysis profiles soundings generally do not sufficiently characterize the inversions. The comparisons showed that the altitudes derived with the CERES lapse-rate technique yield cloud heights that are typically within about 300 m of the cloud base or top (Garreaud et al. 2000). Uncertainties in cloud-top pressure can be determined from the altitude differences in Table 1.

Cloud optical depth, effective particle size - These parameters were also evaluated using retrievals of the same quantities from surface-based instruments at the ARM site using the techniques of Dong et al. (1997) and Mace et al. (1998). Only single-layered stratus and cirrus clouds were considered. The surface-based cirrus retrieval method is limited to optically thin clouds and loses reliability for clouds with visible optical depth of 3 or more. In one of the 4 daytime cases, the surface retrieval has an optical depth of 4.3. If that point is removed, the mean size and optical depth differences are 2.8 µm and 0.4, respectively. The cirrus comparisons must be performed with extreme caution because of the variability of cirrus. The optical depths derived from VIRS are restricted to roughly 10 or less at night because of the limitations of infrared retrievals. The number of samples found in this initial study is too small, therefore, many additional comparisons are needed. These estimates of error will become more reliable as additional Edition1 VIRS data are processed and as more of the ARM cloud data become available.

Table 1: Uncertainties in cloud parameters based on comparisons at the ARM SGP site.

	Mean difference (VIRS - ARM)	**Standard deviation**	**Standard deviation of difference (%)**	**N**
DAY				
Thick cloud temperature vs mean	1 K	1.6 K	-	12
Thin cloud temperature vs mean	-4.4 K	12.9 K	-	35
Thin cloud height vs mean	0.2 km	1.8 km	-	12
Thin cloud height vs top	-1.1 km	2.0 km	-	12
Thick cloud height vs mean	0.6 km	1.2 km	-	35
Thick cloud height vs top	-0.4 km	1.6 km	-	35
Stratus optical depth	-1.1	4.1	21	19
Stratus effective radius	-0.6	1.8 µm	20	19
Liquid water path	-14.0 gm^{-2}	29 gm^{-2}	25	19
Cirrus optical depth	0.7	1.0	38	4
Cirrus effective diameter	-20.4 µm	20.6 µm	28	4
Ice water path	-5.2 gm^{-2}	18.3 gm^{-2}	31	4
NIGHT				
Thin cloud temperature vs mean	1.2 K	9.2 K	-	29
Thick cloud temperature vs mean	-4.0 K	7.7 K	-	22
Thin cloud height vs mean	0.3 km	1.4 km	-	29
Thin cloud height vs top	-0.8 km	1.5 km	-	29
Thick cloud height vs mean	1.0 km	1.1 km	-	22
Thick cloud height vs top	-0.1 km	1.0 km	-	22
Stratus optical depth	-15.2	12.7	51	12
Stratus effective radius (µm)	-0.9 µm	2.2 µm	26	12
Cirrus optical depth	0.7	1.1	78	8
Cirrus effective diameter (µm)	-14.7 µm	20.0 µm	32	8

Return to Quality Summary for: SSF TRMM Edition1 | SSF TRMM Beta2